Surface-state conduction through π-bonded chains

Katsuyoshi Kobayashi
Department of Physics, Faculty of Science, Ochanomizu University, 2-1-1 Otsuka, Bunkyo-ku, Tokyo 112-8610, Japan
(Received 12 February 2003; published 14 August 2003)

The surface-state conduction of the (111)2×1 surfaces of group-IV semiconductors is studied theoretically. The conductance between the surfaces and a single tip or double tips is calculated using the Landauer formalism. The calculated conductance shows strong site dependence and polarity asymmetry in the cases of the Si and Ge surfaces. But they do not appear in the case of the diamond surface. These differences in the conduction properties reflect the difference in the buckling of the topmost atoms of the π-bonded chain structures. The double-tip conductance shows directional anisotropy which is reduced by the buckling.

DOI: 10.1103/PhysRevB.68.075308 PACS number(s): 73.20.At, 73.23.Ad, 81.05.Cy, 68.37.Ef

I. INTRODUCTION

In recent decades, the understanding of the microscopic electrical transport has remarkably progressed. The quantum-mechanical transport on the submicron scales has extensively been studied in the field of mesoscopic systems[1–3] and the properties of the atomic-scale electrical conduction have been revealed by scanning tunneling microscopy (STM).[4] Examples of the advances in recent years are the direct measurement of the conductance through single molecules[5] and through atomic wires with simultaneously monitoring the atomic structures.[6] In these experiments, the distances between probes are fixed or varied at best by one order.

If we try to investigate the electrical transport continuously from the macroscopic to microscopic scales, the experimental method using microscopic multiprobes is a promising tool.[7–11] In these experiments, probes are contacted in parallel on the surfaces of materials and currents flow laterally between probes. In such a configuration, the electrical conduction becomes more sensitive to the electronic states of surface regions with decreasing the probe distances. At extremely short distances, most currents may flow through the conduction channels specific to surfaces. From this point, it is important to clarify the properties of the conduction through surface states and we have presented theoretical studies on the ballistic conduction through surface states in previous papers.[12–14]

In the first paper, we studied the conduction through Tamm surface states using a simple model and discussed the following points.[12] One is the mechanism of the observation of surface states in STM, which was an unsettled problem.[15,16] Second is the conduction across steps of surfaces, where the differences between surface states and bulk states were clarified. Third are the conduction properties in double-tip systems. We found also that the important factors determining the surface-state conduction are the localization strength of wave functions and the bandwidths of surface-state bands.

In the second paper, we studied the conduction through the Shockley surface states using an sp-hybridized chain model.[13] We solved analytically the wave functions and showed how the localization properties of the wave functions depend on the physical quantities determining the bulk bands. We found that density of states (DOS) is more important than group velocity in the ballistic conduction.

In these studies, we used simple models in order to see the physical quantities determining the surface-state conduction as clearly as possible by reducing the number of parameters. However, the surface states of real surfaces are not simple as these models. Therefore, in this paper, we study the surface-state conduction of more realistic surfaces. Among the realistic surfaces, we choose the (111)2×1 surfaces of group-IV semiconductors because they have relatively simple structures.

The (111) surfaces of group-IV elements are fundamental surfaces and have extensively been studied so far. A famous example is the Si(111)7×7 reconstructed surface. While this reconstruction is the most stable structure among Si(111) surfaces, the surface cleaved at room temperature shows a metastable 2×1 reconstruction. It is now established that the atomic structure of the Si(111)2×1 surface is explained by the π-bonded chain model proposed by Pandey.[17] It is also known that the (111)2×1 surfaces of other group-IV elements, diamond, Ge, α-Sn also have the π-bonded chain structure.[18,19]

The π-bonded chain structure is characterized by the zigzag chains in the top two layers. The zigzag chain of the top layer consisting of two atoms in a surface unit cell is buckled in the cases of the Si and Ge surfaces, but not in the case of the diamond surface. With increasing the buckling amplitude, the band gap in the surface-state bands increases and the atoms of the top layer are ionized by the charge transfer between them. The absence of buckling in the diamond surface is explained by the strong intraatomic Coulomb repulsion preventing the charge transfer.[20] In other picture, the strong covalent bonding of diamond excels the energy gain of occupied surface-state bands lowered by buckling. There is a chemical trend in buckling strength from diamond to Ge[18] including Sn.[19]

Up to now the atomic structures and electronic band structures of the π-bonded chain surfaces have extensively been studied. But the properties of the electrical conduction of these surfaces were scarcely known. So we study the electrical conduction through the π-bonded chains in this paper. A main interest in this study is to clarify the differences and similarities in the surface-state conduction among the group-IV elements. Since the buckling strongly affects the surface states, we expect that the surface-state conduction is sensitive to the buckling strength. The method of calcula-

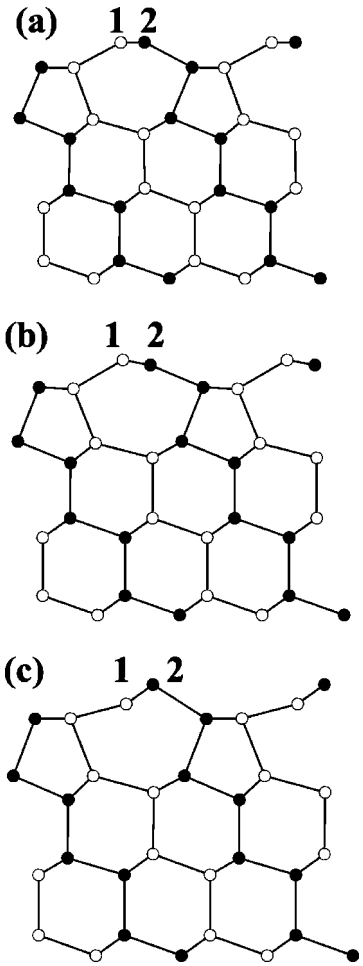

FIG. 1. Side views of atomic structures of the diamond (a), Si (b), and Ge (c) (111)2×1 π-bonded chain surfaces. Open and closed circles show the positions of the atoms on the same planes. Labels 1 and 2 denote the numbers of the topmost chain atoms used in this paper. While the topmost atoms of the diamond surface do not buckle, those of the Si and Ge surfaces buckle in the chain-right and chain-left structures, respectively.

tions is shown in Sec. II. The numerical results and discussions are presented in Sec III.

II. METHOD OF CALCULATION

The method of numerical calculations is similar to those used in the previous studies of the surface-state conduction.[12–14] We consider systems consisting of a surface and a single STM tip or double STM tips, and calculate the conductance of them using the Landauer formalism.[1–3]

The surfaces studied in this paper are the diamond, Si, and Ge (111)2×1 surfaces in the π-bonded chain structures. The atomic structures of these surfaces are shown in Fig. 1. We use the atomic positions obtained by a simulation using an empirical potential for the diamond surface,[21] by a low-energy electron-diffraction experiment for the Si surface,[22] and by a density-functional calculation for the Ge surface.[23] In the cases of the Si and Ge surfaces the topmost chain atoms are buckled and there are two isomers called chain-right and chain-left structures.[23] Density-functional calculations show that the differences in the surface energy between the isomers are very small.[18] A comparison of quasiparticle calculations in the *GW* approximation with experimental data suggests that the Si and Ge surfaces have the chain-right and chain-left structures, respectively.[24] So we assume these structures for the Si and Ge surfaces in this paper. In the case of the diamond surface, the chain-right and chain-left isomers are identical structures due to the absence of buckling.

The electronic states of the surfaces are expressed using the sp^3s^* tight-binding method,[25] in which, in addition to the minimal one *s* and three *p* orbitals, an additional *s* orbital denoted by s^* is introduced in order to express accurately the conduction bands of the bulk semiconductors in the diamond and zinc-blende structures.

At present, it is possible to calculate the electronic states of these surfaces by more sophisticated methods such as the density-functional method. However, it has not yet been established to calculate the electrical conductance through surface states on nanoscales by the density-functional method. There are more accurate tight-binding methods taking account of the interactions beyond nearest neighbors. However, these methods are intended mainly for the bulk electronic states and the parameterizations for the π-bonded surfaces are not known. The purpose of the present paper is not to calculate quantitatively the electrical conductance but to clarify the qualitative difference in surface-state conduction among the group-IV semiconductor surfaces. Therefore, it is enough to express qualitatively the electronic states of these surfaces. Furthermore, we are interested in the electrical conduction on nanoscales such as the double-tip system. Therefore, it is desirable to reduce the basis or parameters expressing the electronic states of the surfaces in order to calculate the conduction of systems as large as possible. So we use the sp^3s^* tight-binding method in this paper.

Figure 2 shows the band structures of the diamond, Si, and Ge(111)2×1 surfaces calculated by the sp^3s^* method. In the surface band calculations, we use slabs consisting of ten double layers. The atoms below the third double layer are placed in the atomic positions of the bulk crystals. The transfer energies between the atoms in the positions different from the ideal bulk ones are calculated using the law by Harrison[26] where the transfer energy is inversely proportional to the square of the interatomic distance. We neglect the transfer energies between the atoms when the distances between them are larger than 1.2 times of the bulk bond lengths. This satisfies the condition that the coordination numbers of the topmost chain atoms and others are three and four, respectively. The dangling bonds on the reverse sides of the slabs are terminated with hydrogen atoms in order to remove the surface states which appear in the fundamental band gaps and are localized at the reverse sides.

In the band calculations, we slightly change the tight-binding parameters and atomic positions in order to fit better the band structures obtained by density-functional calculations. In the diamond surface, the on-site energies of the outermost chain atoms are uniformly shifted by -2.0 eV in order to adjust the positions of the surface-state bands with respect to the bulk ones. In the Si surface, the on-site ener-

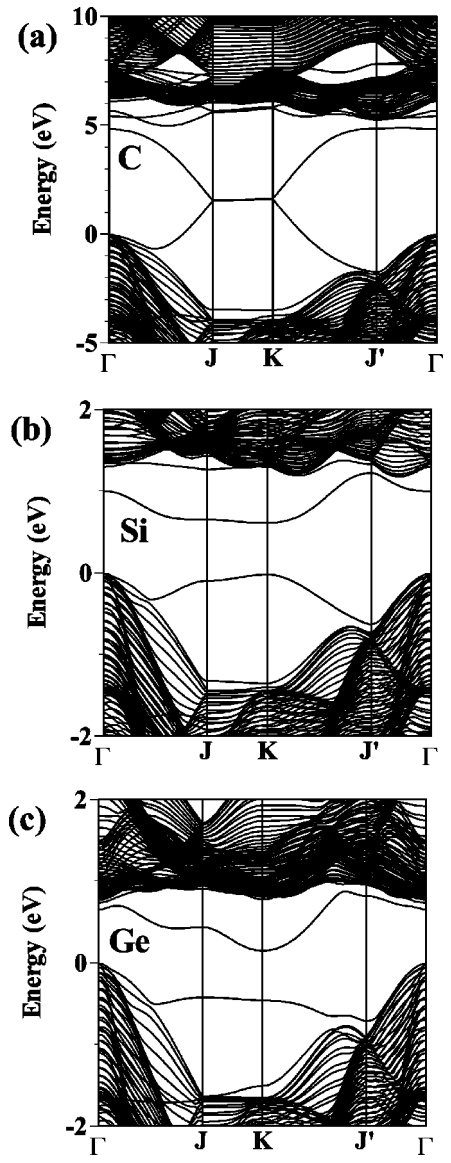

FIG. 2. Band structures of the diamond (a), Si (b), and Ge (c) surfaces calculated by the sp^3s^* tight-binding method. The zero in energy corresponds to the top of the bulk valence bands.

gies of atoms 1 and 2 are shifted by -0.45 and -0.8 eV, respectively, and the buckling of the chain atoms is increased by lifting and lowering the positions of the upper and lower atoms, respectively, by 0.08 Å perpendicular to the surface, in order to adjust the buckling amplitude to that obtained by a recent first-principles calculation.[18] In the Ge surface, the atoms in the second layer are shifted in the [121] direction by 0.1 Å. In the band structure of the Ge surface, the states localized at the reverse side of the slab are removed.

The calculated band structures reproduce the features in the band structures obtained by the density-functional calculations in the local-density approximation for the C,[18,20,27–29] Si,[18] and Ge[18,23] surfaces, and by the quasiparticle calculations in the *GW* approximation for the Si[30,31] and Ge[24,32] surfaces. Though the surface band structures calculated by the sp^3s^* tight-binding method do not quantitatively agree with the first-principles ones, we use them in the calculations of conductance, because as stated above we discuss the properties of the surface-state conduction not depending on the quantitative details of the band structures. The main conclusions in this paper does not qualitatively change even if the tight-binding parameters are slightly varied.

In the surface electronic states, we do not take account of the surface band bending. The band-bending effect appears in various aspects of STM measurements. However, the main interest in this paper is the conduction through surface states. Since the wave functions of surface states are localized within a few layers of surfaces, it can be expected that the band-bending effect is not so important in the surface-state conduction.

The method of calculating the surface-state conductance is described in previous papers.[12–14] Since we are interested in the transport properties on nanoscales, we use the Landauer formalism. In the Landauer formalism, conductance G is given by

$$G = G_0 \sum_{\mu\nu} T_{\mu\nu}, \tag{2.1}$$

where $T_{\mu\nu}$ is the transmission probability from the μth incident channel to the νth scattered channel. G_0 is the quantized conductance unit $2e^2/h$.

In the single-tip case, we calculate the transmission probability from the tip to the surface. In the double-tip case, we consider the situation that the surface is connected with an electrode independent of the two tips. The chemical potential of the first tip injecting electrons into the surface is higher than that of the surface, and that of the second tip is equal to the surface chemical potential. So a part of the electrons injected by the first tip into the surface is ejected through the second tip and the remaining electrons go out through the electrode connected with the surface. Then, we calculate the transmission probability from the first tip to the second tip as well as to the surface.

We use a single atomic chain as a model of the tip. Though this may not be a realistic model for STM tips, we use it for following reasons. First, in the usual experimental situation observing normal STM images, the transmission between a surface and the atom at the apex of an STM tip is most important and the electronic states of the remaining part of the tip is not essential. Second, since we are interested in the nanoscale transport in surfaces, it is desirable to lighten the load in the numerical calculation of the tip by using a tip model as simple as possible.

We assume that there is only one s orbital in each atom of the tip. The on-site and transfer energies are fixed at the top of the valence bands of the surfaces and -5 eV, respectively. All the transfer energies between the apex atom of the tip and the s, p_z, s^* orbitals of the surface atom connected with the tip are -0.5 eV, where z is the direction perpendicular to the surface. As shown in the numerical results of the following section, this tip-surface interaction yields conductance values corresponding to the point-contact measurements rather than the usual STM experimental situations. In actual measurements of the surface-state conduction, the point-contact condition may be useful because large currents im-

prove sensitivity. Since the point-contact condition is assumed, it is not necessary to take account of the energy dependence of the tip-surface interaction which is important in the tunneling condition because the tunneling probability depends exponentially on the square root of energy.

In order to calculate the transmission probability, we solve the Schrödinger equation on appropriate boundary conditions. The wave function of the tip injecting electrons is expressed by linear combination of an incident wave and a reflected wave. The wave function of the second tip in the double-tip case has only an outgoing wave. We impose the boundary condition of outgoing waves on the surface. In particular, in order to calculate unambiguously the surface-state conduction, we impose it on the directions parallel to the surface. For this, we define an imaginary hexahedral region in the surface.[12–14]

The size of the imaginary region is a $N_1 \times N_2 \times N_3$ supercell of the unit cell, where N_1 and N_2 are the numbers of cells parallel to the surface and N_3 is that perpendicular to the surface. We impose the boundary condition of outgoing waves on the five faces of the hexahedron except for one facing the vacuum.

The outgoing waves are obtained by solving generalized eigenvalue problems of wires, where the cross section of a wire is the same as that of each face of the hexahedron.[14] Bloch waves are usually obtained by diagonalizing the transfer matrix which is defined by matrices expressed by using the on-site energies and transfer energies in the tight-binding methods. In the present case, since the determinant of the matrix expressed by the transfer energies is zero, the transfer matrix cannot be defined. Therefore, instead of the transfer matrix, we define a generalized eigen problem and obtain the Bloch states by solving it.[14] Since the determinant is zero, there are solutions that the eigenvalue or its inverse is zero. We discard them and consider only the solutions with nonzero and finite eigenvalues. Outgoing Bloch states are selected out by calculating the group velocity. By imposing the boundary conditions above the Schrödinger equation of the tip-surface systems is reduced to a finite coupled linear equation and the transmission probability is obtained by solving it.

III. NUMERICAL RESULT

A. Single tip

Figure 3 shows calculated conductance spectra. The lateral and vertical sizes of the imaginary hexahedral region are a 4×7 super cell of the 2×1 surface unit cell and five double layers, respectively. The tip is put on the topmost chain atoms nearest to the center on the surface of the imaginary region. Solid and dotted lines show the spectra when the tip is put on the chain atoms labeled by 1 and 2 in Fig. 1, respectively.

In the case of the diamond surface, the conductance spectra of the tip positions on the atoms 1 and 2 are almost the same and show the one-dimensional DOS feature having peaks at -2.4 and 3.2 V. On the other hand, the spectra of the Si and Ge surfaces depend strongly on the tip position. This difference reflects the difference in buckling of the

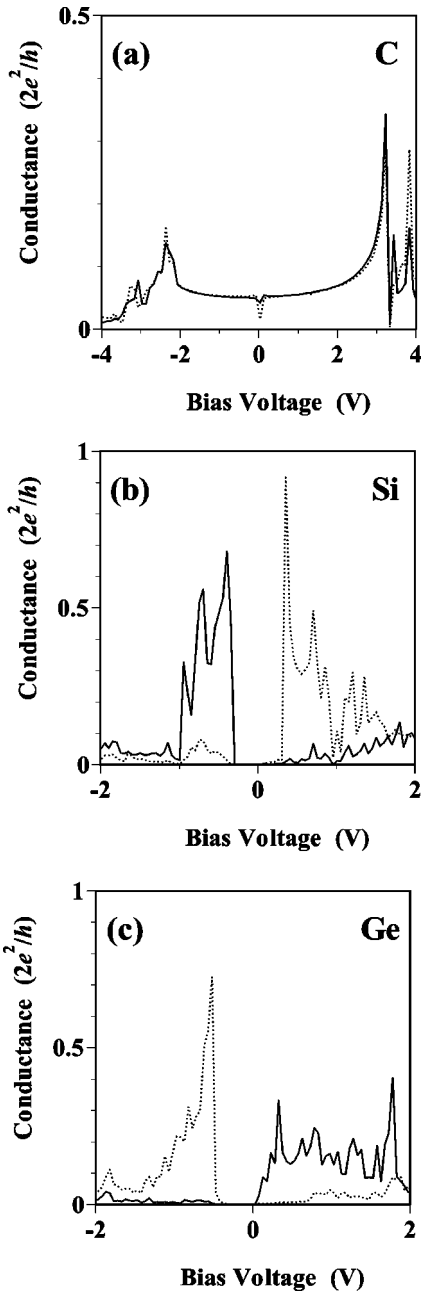

FIG. 3. Single-tip conductance spectra of the diamond (a), Si (b), and Ge (c) surfaces. Solid and dotted lines show spectra when a tip is put on the topmost atoms labeled by 1 and 2 in Fig. 1, respectively.

π-bonded chains. When the tip is put on the atom 1 of the Si surface, conductance is large and small in the energy regions of the occupied and unoccupied surface-state bands, respectively. In the case of the atom 2, the dependence on polarity is reverse. The spectra of the Ge surface show features similar but reverse to those of the Si surface. This is because we assume the chain-right and chain-left isomer structures for the Si and Ge surfaces, respectively. In both surfaces, the conductance of the occupied states is large when the tip is put on the atom shifting to the vacuum side by buckling. The asymmetry between the occupied and unoccupied states in the spectra of the Ge surface is larger than that of the Si

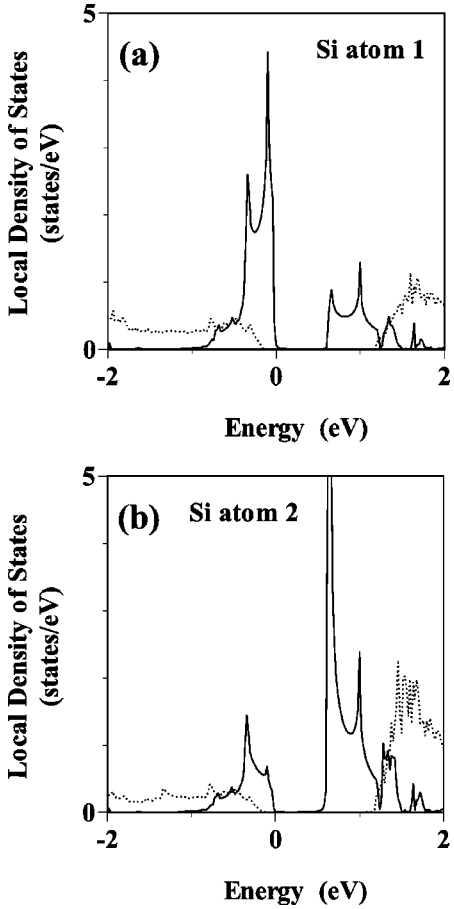

FIG. 4. The LDOS of the Si surface at the atom 1 (a) and 2 (b) shown in Fig. 1. Solid and dotted lines show the surface-state and bulk-state components, respectively.

surface. This reflects the fact that the buckling amplitude of the Ge surface is larger than that of the Si surface and the wave functions localize more on either atom of the topmost chain atoms.

The STM images of the Si and Ge surfaces were obtained experimentally,[33–35] where the asymmetry of the bright spots between the occupied and unoccupied states was clearly observed on both the surfaces. The local conductance spectra of these surfaces were also measured directly by using scanning tunneling spectroscopy (STS), but the asymmetry of polarity is not seen in the STS spectra. This may be due to the artifact of normalization. In the measured conductance spectra, the energy dependence of the transmission probability between a surface and a tip was larger than the energy dependence of DOS and the structures in DOS were not clear. In order to extract the structures in DOS, the conductance spectra dI/dV were normalized by I/V. It can be thought that this normalization hides the polarity asymmetry. If the transmission-probability factor is properly extracted from the conductance spectra, the spectra may show the polarity asymmetry.

Figure 4 shows the local DOS (LDOS) at the topmost chain atoms of the Si surface. The LDOS is obtained from the band calculations shown in Sec. II. Solid and dotted lines show the surface-state and bulk-state components, respectively, which are discriminated by using an effective decay constant $\mu_{\rm eff}$ of a wave function defined by

$$\mu_{\rm eff}=\frac{1}{2}\ln\left(1+\frac{1}{w_n(\mathbf{k}_\parallel)}\right), \tag{3.1}$$

where $w_n(\mathbf{k}_\parallel)$ is a delocalization factor defined by

$$w_n(\mathbf{k}_\parallel)=\sum_{l=1}^{\infty}\sum_{\nu}|C_{nl\nu}(\mathbf{k}_\parallel)|^2(l-1). \tag{3.2}$$

In the above, n and $\mathbf{k}_\parallel$ are a band index and a two-dimensional wave vector in the surface Brillouin zone, respectively. $C_{nl\nu}(\mathbf{k}_\parallel)$ is a coefficient of the νth atomic orbital in a surface unit cell of the lth double layer numbered from the outermost surface layer. The effective decay constant of bulk states calculated using a finite slab with a thickness of N layers is not zero but $\sim 1/N$. Therefore, we judge that when the effective decay constant is larger than $2/N$, the state is a surface state.

A comparison between the conductance spectra and LDOS shows that the conductance spectra are roughly proportional to the LDOS. It is well known that the tunneling conductance between an STM tip and a sample surface is proportional to the LDOS of the sample surface.[36] However, it is not obvious whether this result holds for the surface-state conduction also because the current paths in a sample are different between the bulk and surface conductions. Though the LDOS of surface states is finite at surfaces, there are cases where conductance is zero because surface states are waves not propagating perpendicular to surfaces. This arose a question about the mechanism of the surface-state observation in STM.[15,16] In order to discuss the mechanism of the surface-state observation, we calculated the surface-state conductance in previous papers[12–14] and found that the surface-state conductance is qualitatively proportional to the LDOS if there are conduction paths that allow current to flow laterally. The present result reconfirms the results of the previous papers.

The LDOS shows asymmetry between the valence and conduction bands, which is similar to the conductance spectra. But the strength of the asymmetry in the LDOS is smaller than that in the conductance spectra. Though the figure is not shown, the asymmetry in the LDOS of the Ge surface is also weaker than that in the conductance spectra. In the case of the diamond surface, the asymmetry is not seen in the LDOS and the LDOS's at the two topmost chain atoms are also almost the same, which is similar to the conductance spectra.

The surface-state conductance is higher of the order of the Si, Ge, and diamond surfaces. If the surface-state conductance is proportional to the LDOS, the bandwidth of surface states and the localization strength of wave functions at surfaces are important factors determining the surface-state conductance. In order to clarify the origin of the material dependence of the surface-state conductance, we first investigate the localization strength.

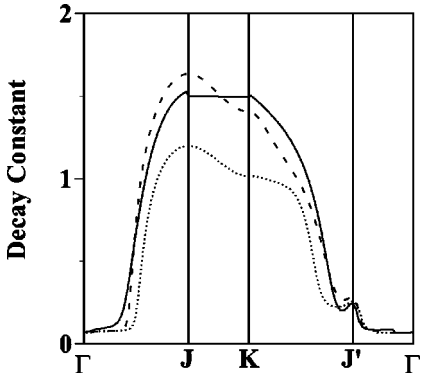

FIG. 5. Effective decay constant μ_{eff} of wave functions of the occupied surface states. Solid, broken, and dotted lines show the effective decay constants of the diamond, Si, and Ge surfaces, respectively.

Figure 5 shows the effective decay constant μ_{eff} defined in Eq. (3.1). The effective decay constants of the occupied surface states are shown. Since μ_{eff} is calculated using finite slabs of ten layers, the regions where μ_{eff} is less than about 0.1 show the bulk states. The effective decay constant of the Ge surface is smaller than those of the diamond and Si surfaces. But the effective decay constants of these surfaces are not much different. Though the figure is not shown, the effective decay constants of the lowest unoccupied surface bands show behavior similar to those of the occupied states. Since the localization strengths of wave functions do not differ much, the difference in the surface-state conductance can be ascribed mainly to the bandwidth factor. The bandwidths of the surface states of the Si and Ge surfaces are narrower than that of the diamond surface. Therefore, the surface-state conductances of the former are larger than that of the latter. This result is contrary to the case of the ideal dangling-bond states,[14] where the localization strength is more important than the bandwidth.

The effective decay constant depends on the parallel wave vector and is large along the *J*-*K* line. In the band structure of the diamond surface, the occupied and unoccupied surface-state bands touch along this line and their energies are located near the center of the bulk band gap. Though in the cases of the Si and Ge surfaces there is a band gap in the surface bands, the surface states along the *J*-*K* line and located also relatively near the center of the bulk band gap. Therefore, there is a tendency that the more surface states are located near the center of the bulk band gap, the stronger their localization. This result is consistent with the argument of the decay constant of the states in bulk band gaps in terms of the complex wave vector.[37]

The effective decay constants of the diamond and Si surfaces are not much different. This result means that the localization strength of the surface states of the π-bonded surfaces is not necessarily related with the bulk band gap. A simple analysis using the nearly free-electron approximation shows that the maximum of the decay constant per layer of a one-dimensional Shockley state is proportional to $E_G a^2$, where E_G and a are a band gap and a lattice constant, respectively.[37] The ratio of $E_G a^2$ is about 6:3:2 for diamond, Si, and Ge. The decay constant of the Shockley state of a one-dimensional sp-hybridized chain model is given by $t_{sp}/\sqrt{|t_{ss}t_{pp}|}$ for small t_{sp}, where t_{ss}, t_{pp}, and t_{sp} are the nearest-neighbor transfer energies between *s* and *s*, *p* and *p*, and *s* and *p* orbitals, respectively.[13] In this model, E_G is proportional to t_{sp}. So if we estimate t_{ss} and t_{pp} by the widths of the valence bands, the ratio of $t_{sp}/\sqrt{|t_{ss}t_{pp}|}$ is also about 6:3:2. These results mean that the localization strength of the surface states of the π-bonded surfaces is not explained by these simple models.

Actually, the localization properties of the ideal dangling-bond states of the (111) surfaces of group-IV semiconductors are not so simple as those of these two-band models.[14] It was shown that the decay constants of the ideal dangling-bond states are expressed by linear combination of the states near the top of the valence bands and the bottom of the conduction bands. Though the states near the top of the valence bands of diamond, Si, and Ge are almost the same, the states near the bottom of the conduction bands are different. For example, in the ideal dangling-bond states at the Γ point in the two-dimensional Brillouin zone, the *p* state at the bottom of the conduction bands is dominant in the case of the diamond surface.[14] But, the *s* state is dominant in the case of the Ge surface, and both the *s* and *p* states are indispensable in the case of the Si surface. This difference in components is reflected on the physical quantities determining the decay constants of wave functions and the localization properties of the ideal dangling-bond states are complicated. Similarly, the decay behavior of the surface states of the π-bonded chain surfaces is not determined by only the bulk band gaps and the interpretation of their localization strength is not simple.

B. Double tips

Figure 6 shows the conductance spectra from the first to the second tip in the double-tip system. The size of the imaginary hexahedral region is the same as the single-tip case. Solid and dotted lines show the conductances when the two tips are positioned parallel and perpendicular to the π-bonded chains, respectively. The first tip is put on the topmost chain atoms nearest to the center of the surface of the imaginary region. The distances from the first to the second tip in the parallel and perpendicular positions are three times the parallel lattice constant and two times the perpendicular one, respectively. The actual parallel and perpendicular distances are 7.5 and 8.7 Å in the diamond surface, 11.5 and 13.3 Å in the Si surface, and 12.0 and 13.9 Å in the Ge surface. So the parallel and perpendicular distances may be regarded as nearly equal. The two tips are put on the equivalent atoms of the π-bonded chains labeled by 1 in Figs. 6(a), 6(c), and 6(e) and by 2 in Figs. 6(b), 6(d), and 6(f).

The double-tip conductance spectra differ from the single-tip ones. An obvious difference is that the double-tip conductance is almost zero outside the energy regions of the surface-state bands. The reason for this is the difference in the contribution of bulk states. In the single-tip case bulk states as well as surface states contribute to conduction channels. But in the double-tip case, the transmission probability from the first to the second tip through bulk states is very small. Most of the conductance is the surface-state conduc-

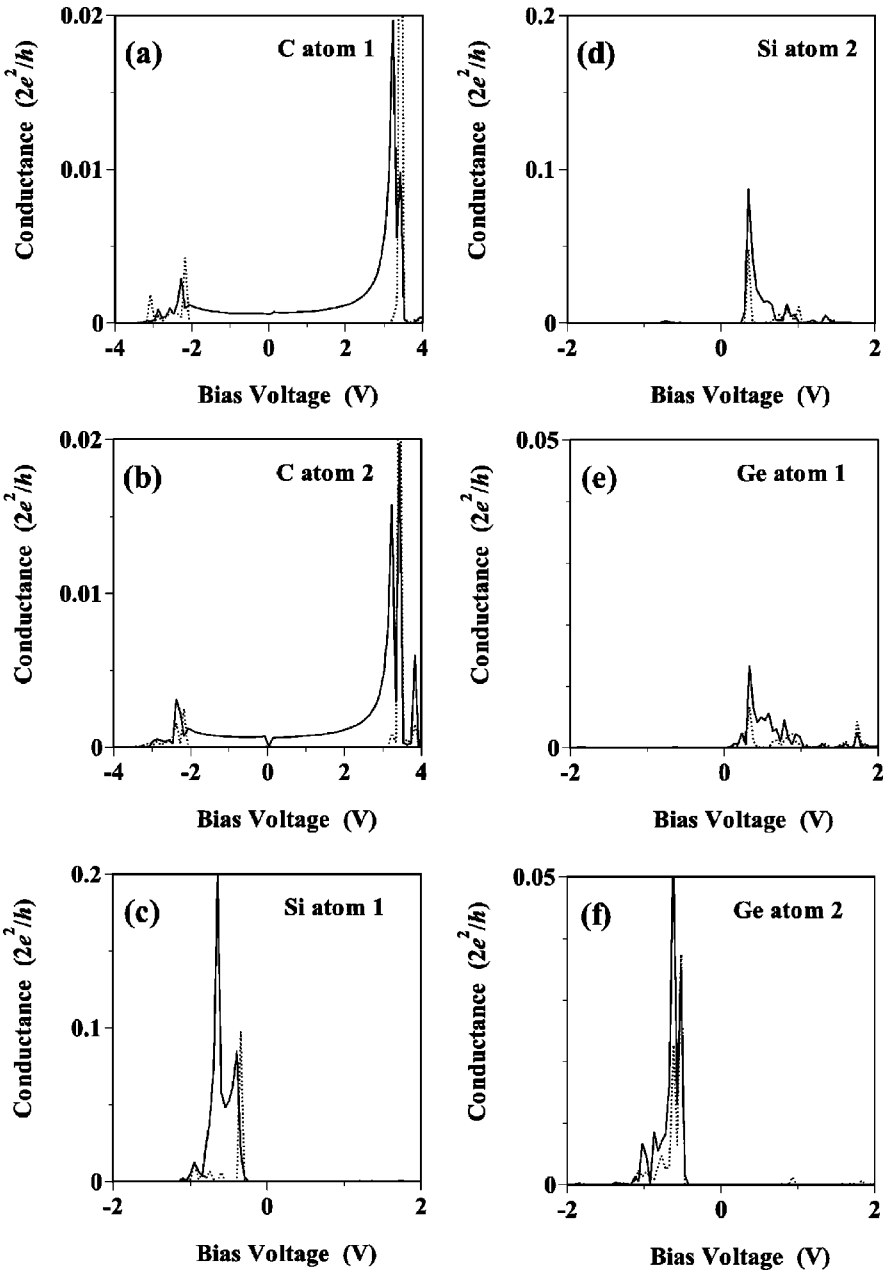

FIG. 6. Double-tip conductance spectra of the diamond (a), (b); Si (c), (d); and Ge (e), (f) surfaces. The first and second tips are put on an atom 1 and another atom 1 in a different unit cell [(a), (c), and (e)] and on atoms 2 [(b), (d), and (f)]. Solid and dotted lines show the conductances when the distances between the two tips are 3 and 2 lattice constants in the directions parallel and perpendicular to the π-bonded chain, respectively.

tion in the ballistic regime. This point has been already discussed in a previous study of the surface-state conduction through Tamm states.[12]

The difference between the single-tip and double-tip conductances is significant in the cases of the Si and Ge surfaces. This is due to the fact that the energy regions where surface and bulk states overlap are large because of the opening of the gaps in the surface-state bands by the buckling. But the single-tip and double-tip conductances are regarded similar if the component of the transmission to bulk states is neglected in the single-tip conductance. Actually, the surface-state components in the LDOS shown in Fig. 4 are similar to the double-tip conductance spectra.

The double-tip conductance shows strong directional anisotropy. In all the surfaces there is a tendency that the conductance parallel to the π-bonded chain is larger than the perpendicular one. The conductance of the diamond surface is highly anisotropic near the zero bias, showing almost one-dimensional conduction. The conduction of the Si and Ge surfaces is less anisotropic than the diamond case, which is closely related with the buckling of the π-bonded chains as discussed later.

The double-tip conductance is qualitatively explained by the Green function of the sample surface. Using the second-order time-dependent perturbation theory Niu *et al.* showed that the double-tip conductance is expressed in terms of the retarded Green function of the sample surface,[38] where the retarded Green function is given by

$$g(\mathbf{r},\mathbf{r}';E)=\frac{\Omega}{(2\pi)^2}\sum_n \int \frac{\phi_{n\mathbf{k}_\parallel}(\mathbf{r})\phi^*_{n\mathbf{k}_\parallel}(\mathbf{r}')}{E-E_n(\mathbf{k}_\parallel)+i\delta}d^2k. \quad (3.3)$$

In the above, $\phi_{n\mathbf{k}_\parallel}(\mathbf{r})$ and $E_n(\mathbf{k}_\parallel)$ are the wave function and the energy of a state in the nth band with a two-dimensional

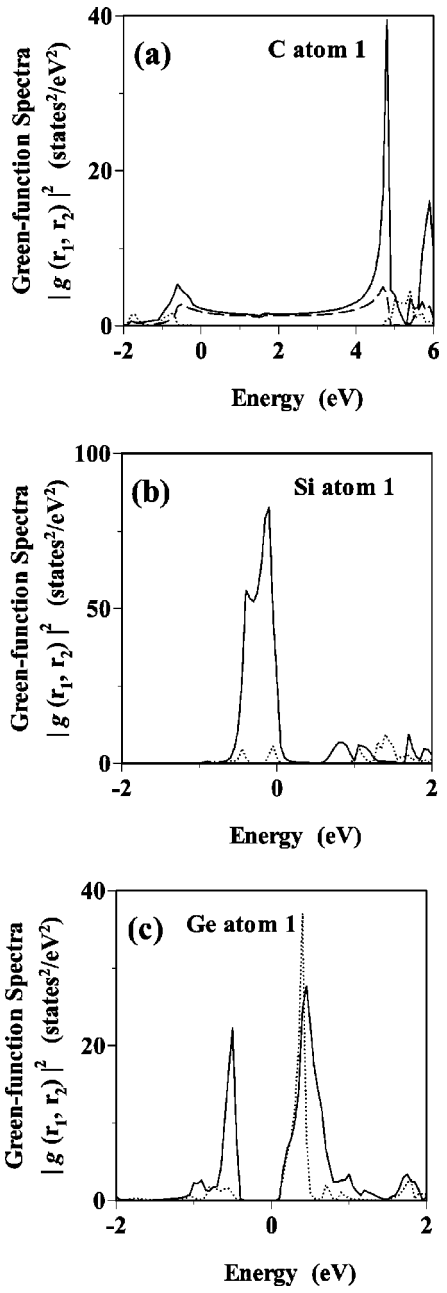

FIG. 7. Green-function spectra of the diamond (a), Si (b), and Ge (c) surfaces. The squared absolute value of the Green function is shown. Both the two positions in the Green function are the sites of atom 1 in Fig. 1. Solid and dotted lines show the spectra when the distances between the two positions are 3 and 2 lattice constants in the directions parallel and perpendicular to the π-bonded chain, respectively. Broken line in (a) shows the spectrum when the distance is ten lattice constants in the parallel direction.

wave vector $\mathbf{k}_\parallel$ parallel to the surface. Ω is the area of the two-dimensional unit cell and δ is a positive infinitesimal. If the interactions between a surface and tips are constant, the double-tip conductance is proportional to the square of the absolute value of the Green function as

$$G \propto |g(\mathbf{r}_1, \mathbf{r}_2; E)|^2, \tag{3.4}$$

where $\mathbf{r}_1$ and $\mathbf{r}_2$ are the positions of the first and second tips on the surface, respectively.

Figure 7 shows the squared absolute value of the Green function. The Green function is obtained from the results of the band calculations of finite slabs in the way similar to the calculations of the LDOS. The Green-function spectra qualitatively reproduce the double-tip conductance spectra. The asymmetry between the valence and conduction bands of the Si and Ge surfaces is seen in the Green-function spectra. But it is weaker than that in the conductance spectra, which is similar to the difference between the LDOS and the single-tip conductance.

A Green-function spectrum for a larger distance between the two tips is shown in the figure of the diamond surface. The positions of the two tips are parallel to the π-bonded chain. Though the heights of the peaks at the edges of the surface-state bands decrease with the distance, the spectrum in the middle part of the surface-state bands does not change much, showing the quasi-one-dimensional conduction. The distance dependence of the Green function varies with materials. Though the figures are not shown, the Green functions of the Si and Ge surfaces decrease faster than the inverse of the distance, which is expected from the behavior of two-dimensional isotropic surface states. These results suggest the difference in dimensionality of the surface-state conduction between the diamond surface and the Si and Ge surfaces.

Next we discuss the anisotropy in the double-tip conductance in details. Figure 8 shows energy spectra of the ratio of the Green function perpendicular to the π-bonded chain to the parallel one. The energy regions shown correspond to the surface-state bands. Though the ratio depends on the energy, it is seen as a whole that the conduction of the diamond surface is highly anisotropic and those of the Si and Ge surfaces are less anisotropic.

In order to clarify the origin of this difference, we discuss qualitatively the conductance anisotropy. We consider an ellipsoidal constant-energy surface as

$$E = \frac{\hbar^2 k_x^2}{2m_x} + \frac{\hbar^2 k_y^2}{2m_y}, \tag{3.5}$$

where m_x and m_y are effective masses of the x and y directions. An asymptotic expression of the Green function for a large distance between two tips is given by Niu *et al.*[38] If we assume that the amplitudes of wave functions of surface states at the surface are the same, the Green function for the ellipsoidal energy surface is given by

$$|g(r,\theta)|^2 \propto \frac{m_x m_y}{r\sqrt{m_x \cos^2\theta + m_y \sin^2\theta}}, \tag{3.6}$$

where r is the distance between tips and θ is the angle between the x axis and the direction of the line connecting the two tips. Furthermore, if we assume that the interactions between a surface and tips are independent of orbitals, the anisotropy of conductance for a fixed distance between tips is given by

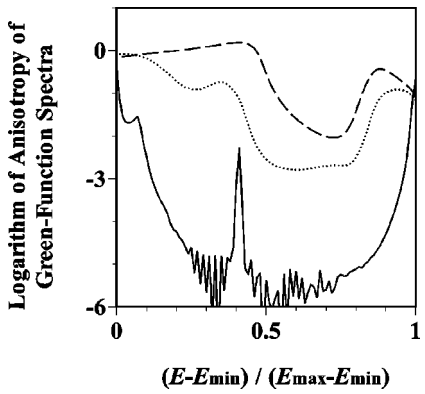

FIG. 8. Anisotropy of the Green-function spectra. The Green-function spectra are given by the squared absolute value of the Green function. The distances between the two positions in the Green function are 3 and 2 lattice constants in the directions parallel and perpendicular to the π-bonded chain, respectively. Anisotropy is expressed by the logarithm of the ratio of the perpendicular spectra to the parallel ones. Solid, dotted, and broken lines show the anisotropy of the diamond, Si, and Ge surfaces, respectively. $E_{\min}$ and $E_{\max}$ are -0.7 and 4.9 eV for the diamond surface, -0.7 and 0.0 eV for the Si surface, and 0.1 and 0.8 eV for the Ge surface.

$$\frac{G_x}{G_y} = \sqrt{\frac{m_y}{m_x}}, \tag{3.7}$$

where G_x and G_y are the conductances when the two tips are positioned parallel to the x and y axes, respectively. This result means that the smaller the effective mass, the larger the conductance, which is the same tendency as the bulk conductivity. The surface-state bands in Fig. 2 show that the dispersions parallel to the chains are larger than the perpendicular ones, which is consistent with the result that the conductances parallel to the chains are larger than the perpendicular ones.

Similar results are expected on other surfaces with anisotropy. For example, the (001) surfaces of group-IV semiconductors are reconstructed in the anisotropic dimer structures. The band dispersions of the surface states in the direction parallel to the dimer row is larger than those in the perpendicular direction. Therefore, it is expected that the conductance parallel to the dimer rows is larger than the perpendicular one. The strong anisotropy of surface states appeared as the quasi-one-dimensional standing-wave formation parallel to the dimer row of the Si(001) surface.[39,40]

Due to the almost one-dimensional conduction, the conductance of the diamond surface is very small when the two tips are put on the neighboring chains apart by only one lattice constant. This makes it difficult to measure the double-tip conductance in real experimental conditions. In such a case, the conductance may be measured by increasing the contact areas of the tips on surfaces instead of the single-atom contact.

The strength of the conductance anisotropy decreases with increasing the amplitude of the buckling. This result may be explained by the wave functions of the surface states as follows. Due to no buckling, the wave functions of the diamond surface extend evenly over the topmost two atoms of the π-bonded chains and there are strong conduction paths along the chains. On the other hand, the wave functions of the Si and Ge surfaces localize more at either site of the topmost two atoms due to the buckling. As a result, the wave functions are isolated along the direction parallel to the chains as well as the perpendicular direction and the conductance anisotropy weakens. Since the localization strength at either site increases with increasing the buckling, the conductance anisotropy also decreases with the buckling. This is consistent with the fact that the band dispersions of the surface states of the Si and Ge surfaces are less anisotropic than those of the diamond surface.

IV. CONCLUSION

We studied theoretically the surface-state conduction on the (111)2×1 π-bonded chain surfaces of group-IV semiconductors. We calculated the ballistic conductance of the single-tip and double-tip systems.

While the single-tip conductance spectra of the Si and Ge surfaces depend on the position of the tip on the two topmost chain atoms and show asymmetry between the occupied and unoccupied states, those of the diamond surface do not depend on the tip position nor show asymmetry. This is due to the difference in the buckling of the chain atoms. The surface-state conductance is qualitatively proportional to the LDOS at the chain atoms. The surface-state conductance is larger of the order of the Si, Ge, and diamond surfaces. It was found that the main factor determining these surface-state conductance of the π-bonded surfaces is the bandwidth of the surface states rather than the localization strength of wave functions. The localization strength of the surface states of the π-bonded chain surfaces is not necessarily proportional to the bulk band gap. This is due to the fact that the properties of Shockley states are determined by bulk states near the top of valence bands and the bottom of conduction bands. In the cases of the group-IV semiconductor surfaces, there are many bulk bands near the bulk band gaps and the surface states are not simple as the two-band models.

The double-tip conductance spectra are different from those of the single-tip ones because most of the conductance in the former is the surface-state conduction. The double-tip conductance of the π-bonded chain surfaces shows anisotropy reflecting the atomic structures. While the conduction of the diamond surface is highly anisotropic and almost one dimensional, those of the Si and Ge surfaces are less anisotropic. The origin of this difference is the buckling. Due to the buckling, the wave functions of the surface states of the Si and Ge surfaces localize more at either site of the topmost two atoms of the π-bonded chains and the conduction recovers the isotropy.

The double-tip conductance spectra are qualitatively reproduced by the Green function of the surfaces. It was shown using an ellipsoidal energy surface that the conductance anisotropy is given by the square root of the inverse of the anisotropy in the effective mass. This result means that the

lighter the effective mass, the larger the conductance, which is similar to the bulk conduction.

In conclusion, the surface-state conduction is strongly influenced by the buckling of the π-bonded chains. The buckling induces asymmetry between the occupied and unoccupied surface states but reduces the directional anisotropy in the double-tip conductance.

ACKNOWLEDGMENTS

Numerical calculations were performed at supercomputers at the Institute of Solid State Physics and the Institute for Molecular Science. This work was partially supported by a Grant-in-Aid from the Ministry of Education, Culture, Sports, Science and Technology, Japan.

[1] S. Datta, *Electronic Transport in Mesoscopic Systems* (Cambridge University Press, Cambridge, 1995).
[2] D. K. Ferry and S. M. Goodnick, *Transport in Nanostructures* (Cambridge University Press, Cambridge, 1997).
[3] Y. Imry, *Introduction to Mesoscopic Physics* (Oxford University Press, Oxford, 1997).
[4] R. Wiesendanger, *Scanning Probe Microscopy and Spectroscopy* (Cambridge University Press, Cambridge, 1994).
[5] M.A. Reed, C. Zhou, C.J. Muller, T.P. Burgin, and J.M. Tour, Science **278**, 252 (1997).
[6] H. Ohnishi, Y. Kondo, and K. Takayanagi, Nature (London) **395**, 780 (1998).
[7] S. Hasegawa, X. Tong, S. Takeda, N. Sato, and T. Nagao, Prog. Surf. Sci. **60**, 89 (1999).
[8] S. Hasegawa, J. Phys.: Condens. Matter **12**, R463 (2000).
[9] C.L. Petersen, F. Grey, I. Shiraki, and S. Hasegawa, Appl. Phys. Lett. **77**, 3782 (2000).
[10] I. Shiraki, F. Tanabe, R. Hobara, T. Nagao, and S. Hasegawa, Surf. Sci. **493**, 633 (2001).
[11] S. Hasegawa, I. Shiraki, T. Tanikawa, C.L. Petersen, T.M. Hansen, P. Boggild, and F. Grey, J. Phys.: Condens. Matter **14**, 8379 (2002).
[12] K. Kobayashi, Phys. Rev. B **65**, 035419 (2002).
[13] K. Kobayashi, Phys. Rev. B **66**, 085413 (2002).
[14] K. Kobayashi and E. Ishikawa, Surf. Sci. **540**, 431 (2003).
[15] C. Noguera, J. Microsc. **152**, 3 (1988).
[16] K. Makoshi, Jpn. J. Appl. Phys., Part 1 **33**, 3657 (1994).
[17] K.C. Pandey, Phys. Rev. Lett. **47**, 1913 (1981).
[18] A.A. Stekolnikov, J. Furthmuller, and F. Bechstedt, Phys. Rev. B **65**, 115318 (2002).
[19] Z.Y. Lu, G.L. Chiarotti, S. Scandolo, and E. Tosatti, Phys. Rev. B **54**, 11 769 (1996).
[20] S. Iarlori, G. Galli, F. Gygi, M. Parrinello, and E. Tosatti, Phys. Rev. Lett. **69**, 2947 (1992).
[21] A.V. Petukhov, D. Passerone, F. Ercolessi, E. Tosatti, and A. Fasolino, Phys. Rev. B **61**, R10590 (2000).
[22] F.J. Himpsel, P.M. Marcus, R. Tromp, I.P. Batra, M.R. Cook, F. Jona, and H. Liu, Phys. Rev. B **30**, 2257 (1984).
[23] N. Takeuchi, A. Selloni, A.I. Shkrebtii, and E. Tosatti, Phys. Rev. B **44**, 13 611 (1991). The atomic positions of the chain left structure shown in Table IV are used.
[24] M. Rohlfing, M. Palummo, G. Onida, and R. Del Sole, Phys. Rev. Lett. **85**, 5440 (2000).
[25] P. Vogl, H.P. Hjalmarson, and J.D. Dow, J. Phys. Chem. Solids **44**, 365 (1983).
[26] W. A. Harrison, *Elementary Electronic Structure* (World Scientific, Singapore, 1999).
[27] A. Scholze, W.G. Schmidt, and F. Bechstedt, Phys. Rev. B **53**, 13 725 (1996).
[28] W.G. Schmidt, A. Scholze, and F. Bechstedt, Surf. Sci. **351**, 183 (1996).
[29] G. Kern, J. Hafner, and G. Kresse, Surf. Sci. **366**, 445 (1996). Obviously Figs. 5 and 7 are exchanged.
[30] J.E. Northrup, M.S. Hybertsen, and S.G. Louie, Phys. Rev. Lett. **66**, 500 (1991).
[31] M. Rohlfing and S.G. Louie, Phys. Rev. Lett. **83**, 856 (1999).
[32] X. Zhu and S.G. Louie, Phys. Rev. B **43**, 12 146 (1991).
[33] J.A. Stroscio, R.M. Feenstra, and A.P. Fein, Phys. Rev. Lett. **57**, 2579 (1986).
[34] R.M. Feenstra, J.A. Stroscio, and A.P. Fein, Surf. Sci. **181**, 295 (1987).
[35] R.M. Feenstra, Phys. Rev. B **44**, 13 791 (1991).
[36] J. Tersoff and D.R. Hamann, Phys. Rev. B **31**, 805 (1985).
[37] S. G. Davison and M. Stęślicka, *Theory of Surface States* (Oxford University Press, Oxford, 1996).
[38] Q. Niu, M.C. Chang, and C.K. Shih, Phys. Rev. B **51**, 5502 (1995).
[39] T. Yokoyama, M. Okamoto, and K. Takayanagi, Phys. Rev. Lett. **81**, 3423 (1998).
[40] T. Yokoyama and K. Takayanagi, Phys. Rev. B **59**, 12 232 (1999).